

Article

# Thermal Stability, Combustion Behavior, and Mechanical Property in a Flame-Retardant Polypropylene System

Lili Wang <sup>1,2</sup>, Milin Zhang <sup>2</sup> and Baibin Zhou <sup>1,\*</sup>

<sup>1</sup> Key Laboratory of Synthesis of Functional Materials and Green Catalysis, Colleges of Heilongjiang Province, Harbin Normal University, Harbin 150025, China; liliwangsh@gmail.com

<sup>2</sup> College of Material Science and Chemical Engineering, Harbin Engineering University, Harbin 150001, China; zhangmilin@hrbeu.edu.cn

\* Correspondence: rainkiss1014@126.com; Tel.: +86-451-5893-9893

Academic Editor: Giorgio Biasiol

Received: 5 November 2016; Accepted: 27 December 2016; Published: 10 January 2017

**Abstract:** In order to comprehensively improve the strength, toughness, flame retardancy, smoke suppression, and thermal stability of polypropylene (PP), layered double hydroxide (LDH) Ni<sub>0.2</sub>Mg<sub>2.8</sub>Al-LDH was synthesized by a coprecipitation method coupled with the microwave-hydrothermal treatment. The X-ray diffraction (XRD), morphology, mechanical, thermal, and fire properties for PP composites containing 1 wt %–20 wt % Ni<sub>0.2</sub>Mg<sub>2.8</sub>Al-LDH were investigated. The cone calorimeter tests confirm that the peak heat release rate (pk-HRR) of PP-20%LDH was decreased to 500 kW/m<sup>2</sup> from the 1057 kW/m<sup>2</sup> of PP. The pk-HRR, average mass loss rate (AMLR) and effective heat of combustion (EHC) analysis indicates that the condensed phase fire retardant mechanism of Ni<sub>0.2</sub>Mg<sub>2.8</sub>Al-LDH in the composites. The production rate and mean release yield of CO for composites gradually decrease as Ni<sub>0.2</sub>Mg<sub>2.8</sub>Al-LDH increases in the PP matrix. Thermal analysis indicates that the decomposition temperature for PP-5%LDH and PP-10%LDH is 34 °C higher than that of the pure PP. The mechanical tests reveal that the tensile strength of PP-1%LDH is 7.9 MPa higher than that of the pure PP. Furthermore, the elongation at break of PP-10%LDH is 361% higher than PP. In this work, the synthetic LDH Ni<sub>0.2</sub>Mg<sub>2.8</sub>Al-LDH can be used as a flame retardant, smoke suppressant, thermal stabilizer, reinforcing, and toughening agent of PP products.

**Keywords:** polypropylene; layered double hydroxide; mechanical property; thermal stability; flame retardancy; composite

## 1. Introduction

Polypropylene (PP) is extensively used in many fields, including floor coverings, automobiles, building materials, electronics and electric materials, various home textiles, wall-coverings, and so on [1–6]. However, relatively poor thermal stability and fire resistance of PP limit the conditions and range of its practical application [7,8]. In particular, the damage to human life becomes serious because PP always produces CO during combustion [9–12]. To reduce flammability and release of CO, the addition of flame retardants is an effective way [13–17]. Moreover, it is well known, to improve the strength and poor toughness of PP, the reinforcing and toughening agents are necessary additives [18]. Therefore, the addition of a small amount of flame retardant not only can increase the flame retardancy, smoke suppression, and thermal stability, but also can enhance the mechanical property of PP polymer, which is a desired goal in this work.

In the past few decades, many researchers have been focusing on exploiting environmentally-friendly halogen-free fire retardants for PP materials. Inorganic fillers, such as magnesium hydroxide

(MTH) and aluminum hydroxide (ATH), have been widely applied in flame-retardant polymeric materials [19]. These fillers could decrease the temperature of the burning materials by endothermic dehydration reaction and release water vapor into the gas phase to dilute the flame. However, the high loading of inorganic fillers ( $\approx 60$  mass%) is usually required to obtain a satisfactory flame retardancy of PP composites, which leads to the reduction in the processing characteristics and deteriorated mechanical properties of the materials [20,21].

The layered double hydroxides (LDH) materials as a result of their high aspect ratio, can improve mechanical properties of samples to a considerable level [22]. The LDH, also known as brucite-like layered materials, are a large class of anionic clays with a general formula of  $[M^{2+}_{1-x}M^{3+}_x(OH)_2]^{x+}[A^{n-}]_{x/n} \cdot mH_2O$ , where  $M^{2+}$  and  $M^{3+}$  are divalent and trivalent metal cations,  $x = M^{3+}/(M^{2+}+M^{3+})$  molar ratio and  $A^{n-}$  is an  $n$ -valent interlayer anion [23–25]. During combustion, when LDH loses the adsorbed water and interlayer water, combustible products are then diluted and cooled within the flame zone. Meanwhile, the generated char residue and mixed metal oxide can protect the bulk polymer from air exposure and suppress the release of smoke [26–29]. Therefore, LDH has attracted considerable attention as a flame retardant and thermal stabilizer [30–38]. In particular, Wang et al. confirmed that MgAl LDH and CoAl LDH can efficiently improve the flame retardancy of PP [39,40]. In addition, the Ni-based LDH' catalysts are highly active and cost-effective in the partial oxidation and steam reforming of methane to produce  $H_2$  [41,42]. Furthermore, in our previous report, Ni-containing MgAl-LDH showed obviously higher flame retardant efficiency in comparison with MgAl-LDH in the ethylene vinyl acetate (EVA) matrix [32,35]. However, the flame retardancy and smoke suppression of the Ni-containing MgAl LDH in the PP matrix have not been reported. Thus, by considering the advantages of Ni ions in catalysts and flame retardant in EVA, the Ni-containing MgAl LDH can also be expected to improve the comprehensive performance of PP/LDH composites.

Since NiMgAl-LDH containing 0.2 mole Ni cations has never been reported, therefore, a PP composite with 1 wt %–20 wt %  $Ni_{0.2}Mg_{2.8}Al$ -LDH was prepared in the present work. X-ray diffraction (XRD) and morphology of  $Ni_{0.2}Mg_{2.8}Al$ -LDH and PP/LDH composite were characterized. Furthermore, the composite PP/LDH with comprehensive performance including enhanced flame retardancy, smoke suppression, thermal stability, and mechanical properties were obtained in this work.

## 2. Materials and Methods

### 2.1. Materials

All chemicals used in the preparation are analytical grade without further purification. Nickel nitrate (99%), aluminum nitrate (99%), magnesium nitrate (99%), sodium carbonate (99%), and sodium hydroxide (99%) were purchased from Tianjin Kemiou Fine Chemical Reagent Co. (Tianjin, China). PP (H360F, South Korea's SK Corporation, Tianjin, China) is a homopolymer with a density of  $0.9 \text{ g/cm}^3$  and melt flow index of  $12 \text{ g/10 min}$ . Deionized water was made by a Milli-Q pure water apparatus (Shandong Laisuo Technology Co., Jinan, China) in our Lab.

### 2.2. Synthesis of $Ni_{0.2}Mg_{2.8}Al$ -LDH (Layered Double Hydroxide)

The  $Ni_{0.2}Mg_{2.8}Al$ -LDH was prepared by co-precipitation of 1 M  $Ni(NO_3)_2 \cdot 6H_2O$ , 1 M  $Mg(NO_3)_2 \cdot 6H_2O$  and 1 M  $Al(NO_3)_3 \cdot 9H_2O$  (where  $[Ni^{2+}]:[Mg^{2+}]:[Al^{3+}] = 0.2:2.8:1$ ) with vigorous stirring at  $70 \text{ }^\circ\text{C}$ . The solution was adjusted to a constant pH 8.5 by drop-wise addition of  $NaOH$ - $Na_2CO_3$  mixed solution ( $0.6 \text{ M NaOH}$  and  $0.45 \text{ M Na}_2\text{CO}_3$ ). After the titration, a heavy suspension gel was obtained and transferred to the beaker (1 L). Then, the beaker with suspension gel was put in a microwave oven (XH-300A, the maximum power of 1000 W and a frequency of 2.45 GHz, Beijing Xianghu science and Technology Development Co., Beijing, China) and crystallized at  $70 \text{ }^\circ\text{C}$  for 30 min. The obtained precipitate was washed by the deionized water to pH 7, and then filtered. The synthesized sample was dried under air atmosphere at  $70 \text{ }^\circ\text{C}$ .

### 2.3. Preparation of Polypropylene (PP)/LDH Composites

The PP/LDH composites were prepared via the melt blending method at 175 °C in a RM-200A torque rheometer (Harbin University of Science and Technology, Harbin, China) for 6 min with a rotor speed of 80 rpm. In order to obtain the optimum performance of composites, several formulations with the additive amount of Ni<sub>0.2</sub>Mg<sub>2.8</sub>Al-LDH from small to large ratios (1 wt %, 3 wt %, 5 wt %, 7 wt %, 10 wt %, and 20 wt % mass fraction of LDH content) were systematically investigated. The composites are named PP-1%LDH, PP-3%LDH, PP-5%LDH, PP-7%LDH, PP-10%LDH, and PP-20%LDH, respectively.

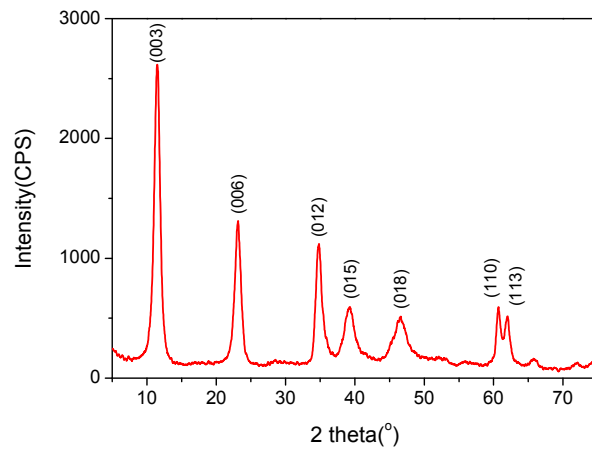
### 2.4. Measurements

X-ray diffraction (XRD) was characterized using a D/MAX 2200 diffractometer (Rigaku, Tokyo, Japan) with  $\lambda = 1.5406 \text{ \AA}$ . Data were collected at the rate of 4°/min and step 0.02° with Cu K $\alpha$  irradiation operated at 40 kV and 45 mA. Scanning electron microscope (SEM) (FEI, Eindhoven, The Netherlands) observations were carried out on a FEI-Sirion with a field emission of 20 kV. The X-ray energy dispersive spectroscopy (EDS) of LDH was obtained by SEM equipped with the energy-dispersive X-ray spectroscopy (EDAX) Genesis (EDAX Inc., Mahwah, NJ, USA) through a spectrum imaging technique. The specimens were examined in a HITACHI 1H-7650 transmission electron microscope (TEM) (Hitachi, Tokyo, Japan) operated at the accelerating voltage of 100 kV. Thermal analysis was carried out with a thermogravimetric (TG) analyzer (TGA pyris 1 from Perkin Elmer, Perkin Elmer Co., Walther M, Boston, MA, USA) using a constant heating rate of 10 °C/min under the pure nitrogen atmosphere from 50 to 800 °C. The weight of the samples was kept within 3–4 mg. All cone calorimeter tests were carried out in a cone calorimeter (FTT0007, Hongkong Universal Technology Co., Hong Kong, China) at an incident heat flux of 50 kW/m<sup>2</sup> according to the ISO 5660-1 standard. The polymer sample (100 × 100 × 5 mm<sup>3</sup>) is placed horizontally on a balance holder. The elongation at break and tensile strength of all samples was performed by a RGD-20A material test machine (produced by Shenzhen Regear Instrument Cooperation, Shenzhen, China), according to the national standard GB/T 16421-1996.

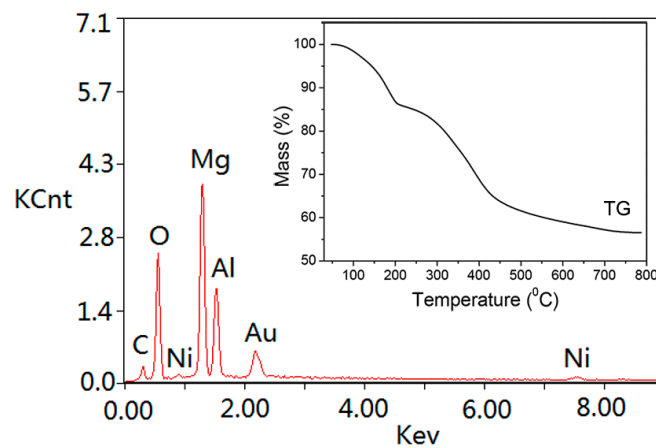
## 3. Results and Discussion

### 3.1. X-ray Diffraction (XRD), Element, and Morphology Analysis of LDH

Figure 1 shows XRD pattern of Ni<sub>0.2</sub>Mg<sub>2.8</sub>Al-LDH. The Ni<sub>0.2</sub>Mg<sub>2.8</sub>Al-LDH exhibit (0 0 3), (0 0 6), (0 1 2), (0 1 5), (0 1 8), (1 1 0), and (1 1 3) characteristic diffraction peaks of the LDH structure, which can be indexed in a hexagonal lattice with an R3m rhombohedral space group symmetry [43,44]. These reflection positions are in good agreement with those of the reported LDHs [43,45]. Figure 2 illustrates the EDS analysis and TG curve of Ni<sub>0.2</sub>Mg<sub>2.8</sub>Al-LDH. From the TG curve, it can be seen that the Ni<sub>0.2</sub>Mg<sub>2.8</sub>Al-LDH mainly underwent two stages decomposition. The first stage corresponds to the loss of physical absorbed water and interlayer water in the range of 50 to 200 °C [46]. The second stage in the range of 200 to 800 °C is associated with the dehydroxylation of the metal hydroxide layers and the degradation of carbonates [47]. The TG analysis showed the mass loss percentages of H<sub>2</sub>O molecules for Ni<sub>0.2</sub>Mg<sub>2.8</sub>Al-LDH. The composition of other elements was obtained using the Leco CHNS-932 elemental analyzer (Leco Co., Saint Joseph, MO, USA) and atomic absorption apparatus (AAS) (Purkinje General Instrument Co., Beijing, China). The chemical formula of the Ni<sub>0.2</sub>Mg<sub>2.8</sub>Al-LDH is Ni<sub>0.16</sub>Mg<sub>2.55</sub>Al(OH)<sub>7.42</sub>(CO<sub>3</sub>)<sub>0.50</sub>·H<sub>2</sub>O<sub>1.53</sub>. This chemical formula is in good agreement with the EDS elemental analysis results. Both AAS test and EDS analysis proved the existence of Ni ions in Ni<sub>0.2</sub>Mg<sub>2.8</sub>Al-LDH.

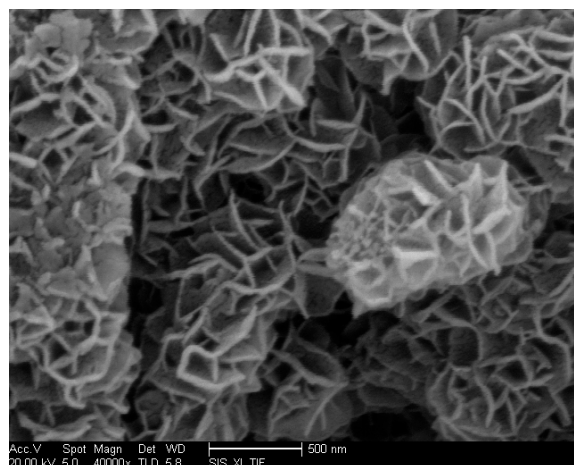


**Figure 1.** X-ray Diffraction (XRD) pattern of  $\text{Ni}_{0.2}\text{Mg}_{2.8}\text{Al-LDH}$ .

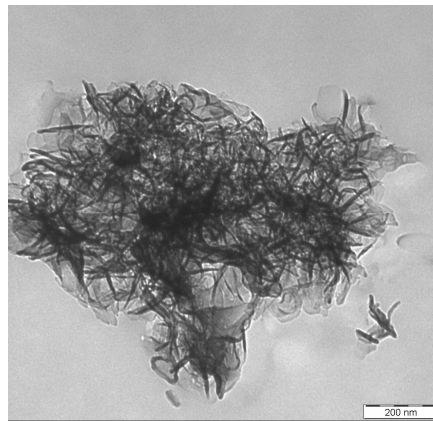


**Figure 2.** X-ray energy dispersive spectroscopy (EDS) and thermogravimetric (TG) curve of  $\text{Ni}_{0.2}\text{Mg}_{2.8}\text{Al-LDH}$ .

Figure 3 shows the SEM image of  $\text{Ni}_{0.2}\text{Mg}_{2.8}\text{Al-LDH}$ . It can be seen that the morphology of  $\text{Ni}_{0.2}\text{Mg}_{2.8}\text{Al-LDH}$  is petal-like sheet particles with many cavities. Furthermore, in order to obtain more fine morphology and particle size, the TEM image of  $\text{Ni}_{0.2}\text{Mg}_{2.8}\text{Al-LDH}$  is shown in Figure 4. As seen from the TEM image,  $\text{Ni}_{0.2}\text{Mg}_{2.8}\text{Al-LDH}$  has a flake nanoparticles morphology.



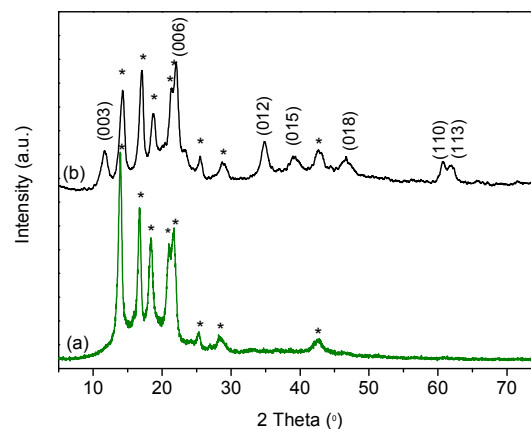
**Figure 3.** Scanning electron microscope (SEM) image ( $40,000\times$ ) of  $\text{Ni}_{0.2}\text{Mg}_{2.8}\text{Al-LDH}$ .



**Figure 4.** Transmission electron microscope (TEM) image (100,000 $\times$ ) of  $\text{Ni}_{0.2}\text{Mg}_{2.8}\text{Al-LDH}$ .

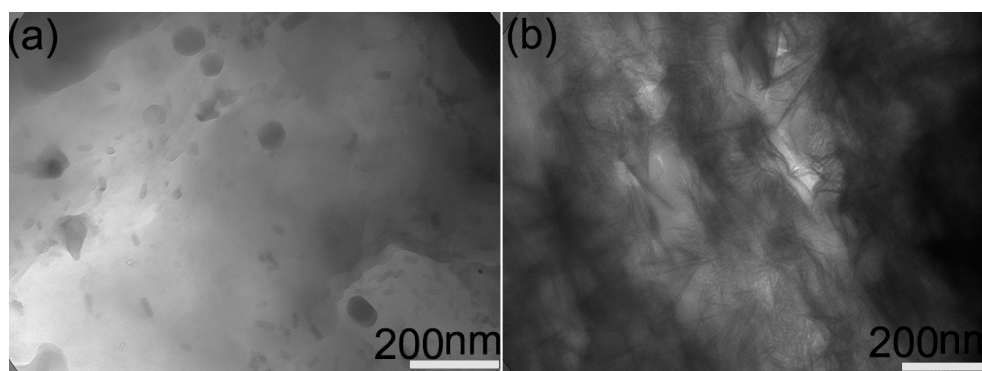
### 3.2. XRD and Morphology Analysis of Composites

Figure 5a,b shows the XRD patterns of the pure PP and composite PP-20%LDH with 20%  $\text{Ni}_{0.2}\text{Mg}_{2.8}\text{Al-LDH}$ , respectively. The XRD pattern of PP-20%LDH shows the characteristic reflections of  $\text{Ni}_{0.2}\text{Mg}_{2.8}\text{Al-LDH}$  and PP. The XRD analysis confirmed that the  $\text{Ni}_{0.2}\text{Mg}_{2.8}\text{Al-LDH}$  is dispersed in the PP matrix. Furthermore, the (003) diffraction peak of  $\text{Ni}_{0.2}\text{Mg}_{2.8}\text{Al-LDH}$  retains its original position in the PP-20%LDH. This result indicates that the intercalation structures of  $\text{Ni}_{0.2}\text{Mg}_{2.8}\text{Al-LDH}$  do not exist in the PP-20%LDH.



**Figure 5.** XRD patterns of the pure polypropylene (PP) and PP-20%LDH; (a) pure PP; and (b) PP-20%LDH. The asterisk represents the diffraction peak of PP.

It is well known that good dispersion of LDH in the polymer matrix can effectively improve the thermal and mechanical performances of the composites [48]. In order to observe the dispersion of the  $\text{Ni}_{0.2}\text{Mg}_{2.8}\text{Al-LDH}$  platelets in the PP matrix, the TEM images at 150,000 times magnification for composite PP-5%LDH and PP-20%LDH were shown in Figure 6a,b, respectively. It can be seen from Figure 6a that a small amount of the intact nano-sized flake  $\text{Ni}_{0.2}\text{Mg}_{2.8}\text{Al-LDH}$  particles are presented in the PP matrix. Therefore, the XRD pattern of PP-20%LDH shows the characteristic reflections of  $\text{Ni}_{0.2}\text{Mg}_{2.8}\text{Al-LDH}$ . At the same time, a large number of small parts with lateral size of 10–40 nm appear in the PP-5%LDH, which are caused by the break of  $\text{Ni}_{0.2}\text{Mg}_{2.8}\text{Al-LDH}$  layers. For PP-20%LDH, the many exfoliated  $\text{Ni}_{0.2}\text{Mg}_{2.8}\text{Al-LDH}$  layers are dispersed disorderly in the PP matrix. The above morphologies observed by TEM can be confirmed that  $\text{Ni}_{0.2}\text{Mg}_{2.8}\text{Al-LDH}$  showed the homogeneous distribution in the PP matrix. Furthermore, the PP-5%LDH and PP-20%LDH composites with the nano-sized filler are the mixed intact flake and exfoliated structures [49].



**Figure 6.** TEM images of composites (150,000 $\times$ ); (a) PP-5%LDH; (b) PP-20%LDH.

### 3.3. Combustion Behavior of Composites

The cone calorimetry method is used to predict the burning behavior of materials in real fire scenarios. All cone calorimeter tests were carried out in a cone calorimeter at an incident heat flux of 50 kW/m<sup>2</sup> according to the ISO 5660-1 standard. Better understanding of the underlying phenomena governing fire initiation and growth has led to the development of HRR test methods. HRR is considered to be a key indicator of fire performance and is the rate at which a material produces energy while burning [50,51]. Simultaneously, the peak value of HRR (pk-HRR) is used to express the intensity of a fire. Figure 7a,b illustrates the heat release rate (HRR) and the production rate of CO<sub>2</sub> (CO<sub>2</sub>P) curves of the pure PP and the composites. The pk-HRR of the pure PP is 1057 kW/m<sup>2</sup>, and the pk-HRR values of PP-5%LDH, PP-10%LDH and PP-20%LDH were obviously decreased to 878, 705, and 500 kW/m<sup>2</sup>, respectively. Liu et al. reported that when 50 mass% ATH is added to the PP matrix, the pk-HRR of PP/ATH composite is 539.8 kW/m<sup>2</sup> [52]. Compared with the reported PP/ATH with 50 mass% ATH, the PP-20%LDH shows better flame retardancy. Furthermore, the pk-HRR time of PP-5%LDH, PP-10%LDH and PP-20%LDH are 295, 340 and 315 s, respectively, which are longer than 245 s of PP. The pk-HRR time of PP/LDH composites were extended, which is more beneficial to people's evacuation and rescue of firefighters. At the same time, a crucial phenomenon was observed. The peak production rate of CO<sub>2</sub> (pk-CO<sub>2</sub>P) time are as accurate same as the pk-HRR time for PP and its composites. This important finding confirmed that the production rates of CO<sub>2</sub> essentially mirror the HRR data. It is consistent with the report of Jiao et al. [53].

Figure 8a-c shows the photographs of residues for composites PP-5%LDH, PP-10%LDH, and PP-20%LDH after cone calorimeter testing, respectively. For PP-5%LDH and PP-10%LDH, the cracked residues can be observed, and the gray substance is mainly the magnesium, aluminum, and nickel mixed oxide, and compounds (NiAl<sub>2</sub>O<sub>4</sub>) produced from the thermal decomposition of Ni<sub>0.2</sub>Mg<sub>2.8</sub>Al-LDH [54]. In comparison with PP-5%LDH and PP-10%LDH, the residues of PP-20%LDH is more intact. It is well known that the continuous and compact residues layers can slow the heat and mass transfer between gas and condensed phases and also protect the underlying materials from further burning. Therefore, the pk-HRR of PP-20%LDH is lower than those of PP-5%LDH and PP-10%LDH. The effective heat of combustion (EHC) is an important parameter to understand how the flame retardant acts. The EHC values of the pure PP, PP-5%LDH, PP-10%LDH, and PP-20%LDH are 34.28, 35.98, 35.36, and 34.34 MJ/kg, respectively. At the same time, the average mass loss rate (AMLR) values of the pure PP, PP-5%LDH, PP-10%LDH and PP-20%LDH are 0.116, 0.100, 0.0928, and 0.0848 g/s, respectively. It can be seen that pk-HRR and AMLR show the gradual decrease with increasing loading of Ni<sub>0.2</sub>Mg<sub>2.8</sub>Al-LDH in the PP matrix. Furthermore, the EHC values of different composites show small changes in comparison with the pure PP. The above pk-HRR, AMLR, and EHC analyses confirmed that the condensed phase fire retardant action of Ni<sub>0.2</sub>Mg<sub>2.8</sub>Al-LDH in the composites, there is nothing significant in the gas phase [55].

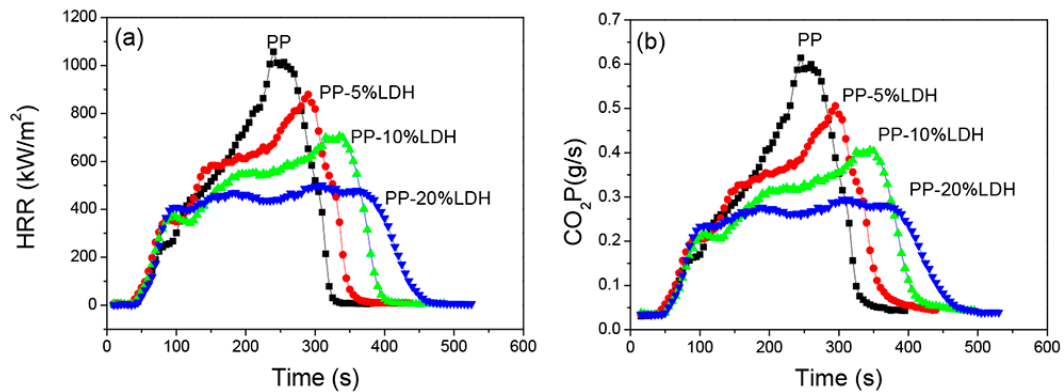


**Figure 7.** Cone calorimetric results of PP and its composites. (a) Heat release rate (HRR) curves; and (b) production rate of CO<sub>2</sub> (CO<sub>2</sub>P) curves.



**Figure 8.** Photographs of residues for composites PP-5%LDH, PP-10%LDH and PP-20%LDH after cone calorimeter testing; (a) PP-5%LDH; (b) PP-10%LDH; and (c) PP-20%LDH.

In addition, it is well known that most deaths result from the toxic gases CO in the case of fire for PP products [9–12]. The production rate of CO (COP) curves are shown in Figure 9. The peak values of COP (pk-COP) for the pure PP, PP-5%LDH, PP-10%LDH, and PP-20%LDH are 0.011, 0.0084, 0.0076, and 0.0043 g/s, respectively. Furthermore, MCOY is the mean release yield of CO of burning materials. The MCOY values of PP, PP-5%LDH, PP-10%LDH, and PP-20%LDH are 0.035, 0.035, 0.034, and 0.029 kg/kg, respectively. The pk-COP and MCOY of composites show obvious decreases with the increase of Ni<sub>0.2</sub>Mg<sub>2.8</sub>Al-LDH in composites. The above cone-calorimetry data show important improvement including both the HRR and the CO suppression of composites in comparison with PP.

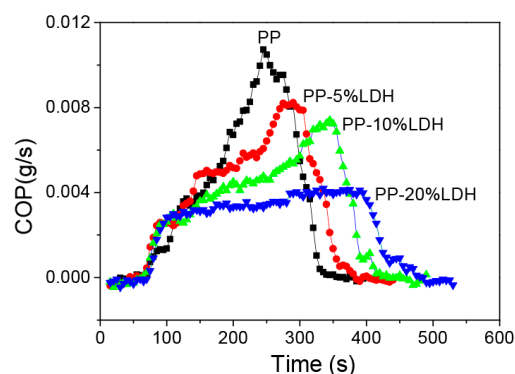


**Figure 9.** Production rate of CO (COP) curves of PP and its composites.

### 3.4. Thermal Analysis of Composites

Figure 10a,b shows the TG and differential thermogravimetry (DTG) curves of the pure PP and its composites, respectively. From the TG curves, it can be seen that the residues mass of

PP-5%LDH, PP-10%LDH, and PP-20%LDH are gradually increased to 3.57%, 6.02% and 10.42% with the increase of  $\text{Ni}_{0.2}\text{Mg}_{2.8}\text{Al-LDH}$  in composites, respectively. The decomposition temperature of PP is at 456 °C in the DTG curves. However, the decomposition temperature of PP-5%LDH and PP-10%LDH reach to 490 °C, which is 34 °C higher than the pure PP. The reason is that the  $\text{Ni}_{0.2}\text{Mg}_{2.8}\text{Al-LDH}$  released  $\text{H}_2\text{O}$  and  $\text{CO}_2$  effectively delay the scission of propylene-based chains. On the contrary, the decomposition temperature of PP-20%LDH is 477 °C, which is decreased compared with PP-5%LDH and PP-10%LDH. The reason is that when the  $\text{Ni}_{0.2}\text{Mg}_{2.8}\text{Al-LDH}$  loading increases to 20 wt %, a lot of metal and metal oxide in turn accelerated the catalytic degradation of PP on heating [56,57].

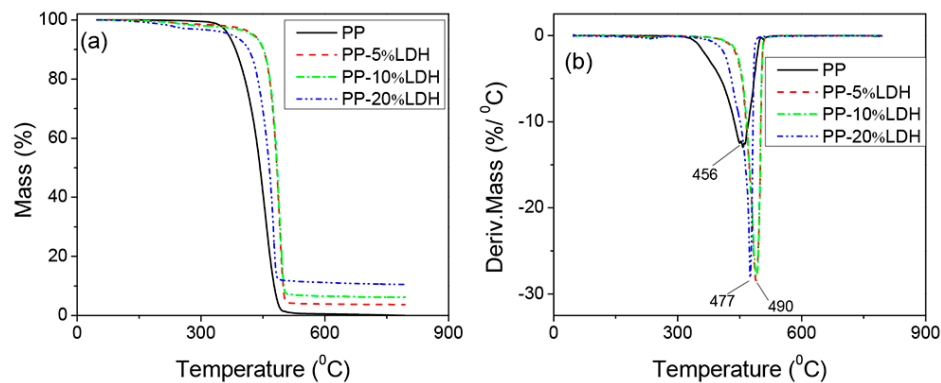


**Figure 10.** Thermogravimetric analysis (TG) and differential thermogravimetry (DTG) curves of PP and its composites; (a) TG curves; and (b) DTG curves. Deriv.: differential of TG curves.

### 3.5. Mechanical Properties of PP and Its Composites

Figure 11a,b shows the tensile strength and the elongation at break of the pure PP and composites. All data points regarding both the tensile strength and the elongation at break are the mean values of 10 test data. Further, the 10 test data are within the error of the measurements. As can be seen from Figure 11a, the tensile strength values of the pure PP, PP-1%LDH, PP-3%LDH, PP-5%LDH, PP-7%LDH, PP-10%LDH, and PP-20%LDH are 12.6, 20.5, 14.4, 15.8, 12.2, 10.6, and 9.7 MPa, respectively. This result indicates that the tensile strength values of PP-1%LDH, PP-3%LDH, and PP-5%LDH are much higher than that of the pure PP, especially PP-1%LDH. As shown in Figure 11b, the elongation at break values of PP-1%LDH, PP-3%LDH, PP-5%LDH, PP-7%LDH, and PP-10%LDH are 761%, 837%, 909%, 922%, and 1015%, respectively. The above elongations at break values are gradually improved with the increase of  $\text{Ni}_{0.2}\text{Mg}_{2.8}\text{Al-LDH}$  in composites. Furthermore, these values are much higher than 654% of the pure PP. In particular, PP-10%LDH is 361% higher than PP. The tensile strength and the elongation at break indicate that  $\text{Ni}_{0.2}\text{Mg}_{2.8}\text{Al-LDH}$  can be used as reinforcing and toughening agents of PP.

It is noteworthy that when  $\text{Ni}_{0.2}\text{Mg}_{2.8}\text{Al-LDH}$  loading reaches 20% in composite, the elongation at break value of PP-20%LDH is decreased to 575%. Simultaneously, the tensile strength values of composites show gradual reduction when  $\text{Ni}_{0.2}\text{Mg}_{2.8}\text{Al-LDH}$  loading is more than 7% in composites. These mechanical test results indicate that the interfacial adhesion between  $\text{Ni}_{0.2}\text{Mg}_{2.8}\text{Al-LDH}$  and the PP matrix is better when a small amount of  $\text{Ni}_{0.2}\text{Mg}_{2.8}\text{Al-LDH}$  was added into composites.  $\text{Ni}_{0.2}\text{Mg}_{2.8}\text{Al-LDH}$  particles and the PP matrix together moved to deformation under the action of external tensile stress. Thus the strength and ductility of the composites were improved because of the increase of the effective interface between  $\text{Ni}_{0.2}\text{Mg}_{2.8}\text{Al-LDH}$  and the PP matrix. However, when  $\text{Ni}_{0.2}\text{Mg}_{2.8}\text{Al-LDH}$  exceed a certain amount, the excessive and agglomerate rigidity particles of  $\text{Ni}_{0.2}\text{Mg}_{2.8}\text{Al-LDH}$  in turn led to a decrease of the tensile strength and ductility of the composites.

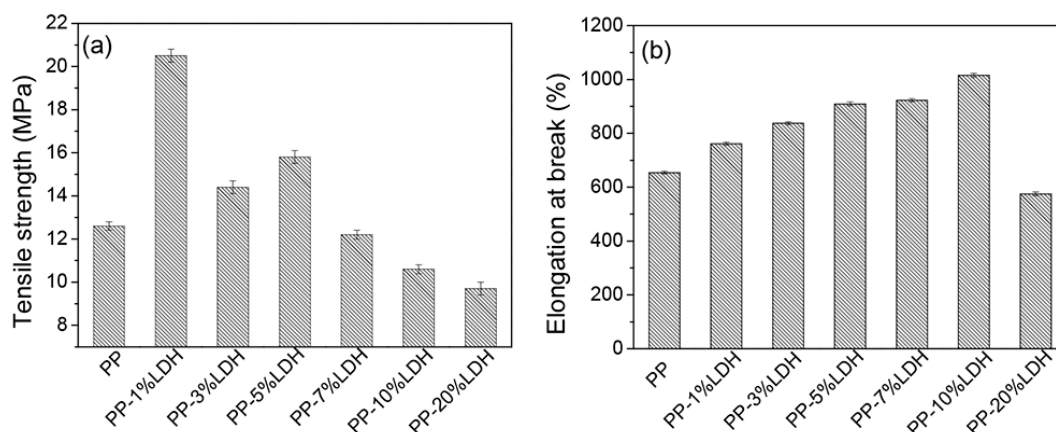


**Figure 11.** Tensile strength and the elongation at break of the pure PP and composites; (a) tensile strength; and (b) elongation at break.

#### 4. Conclusions

XRD and TEM of composites confirm that Ni<sub>0.2</sub>Mg<sub>2.8</sub>Al-LDH was dispersed in the PP matrix. Both the HRR and the CO suppression of composites show important improvements in comparison with that of the PP. The decomposition temperature of PP-5%LDH and PP-10%LDH is 34 °C higher than the pure PP. The tensile strength values of PP-1%LDH, PP-3%LDH and PP-5%LDH are much higher than that of the pure PP. Simultaneously, the elongations at break of the composites with 1 wt %–10 wt % Ni<sub>0.2</sub>Mg<sub>2.8</sub>Al-LDH are higher than that of the PP. This synthetic LDH Ni<sub>0.2</sub>Mg<sub>2.8</sub>Al-LDH can be used as good flame retardant, smoke suppressant, thermal stabilizer, reinforcing and toughening agent of PP products. Furthermore, because the synthesis process of the non-toxic and inexpensive LDH is simple, it is feasible to produce them in large quantity and brings favorable economic benefits.

**Acknowledgments:** This study was financially supported by the National Natural Science Foundation of China (No. 21304014) and the China Postdoctoral Science Foundation Special Funding Project (No. 2014T70308).

**Author Contributions:** The author Lili Wang contributed research and experimental work in this study. The authors Baibin Zhou and Milin Zhang contributed data analysis and revision of this paper.

**Conflicts of Interest:** The authors declare no conflict of interest.

#### References

- Huang, J.; Bian, Z.; Lei, S. Feasibility study of sensor aided impact acoustic sorting of plastic materials from end-of-life vehicles (ELVs). *Appl. Sci.* **2015**, *5*, 1699–1714. [[CrossRef](#)]
- Wang, C.; Li, J.; Ding, P. Roles of supermolecule structure of melamine phosphomolybdate in intumescent flame retardant polypropylene composites. *J. Anal. Appl. Pyrolysis* **2016**, *119*, 139–146. [[CrossRef](#)]
- Huang, C.L.; Lou, C.W.; Liu, C.F.; Huang, C.H.; Song, X.M.; Lin, J.H. Polypropylene/graphene and polypropylene/carbon fiber conductive composites: Mechanical, crystallization and electromagnetic properties. *Appl. Sci.* **2015**, *5*, 1196–1210. [[CrossRef](#)]
- Amieva, E.J.C.; Velasco-Santos, C.; Martinez-Hernandez, A.; Rivera-Armenta, J.; Mendoza-Martinez, A.; Castano, V. Composites from chicken feathers quill and recycled polypropylene. *J. Compos. Mater.* **2014**, *49*, 275–283. [[CrossRef](#)]
- Kumar, R.; Dhaliwal, J.S.; Kapur, G.S. Mechanical properties of modified biofiller-polypropylene composites. *Polym. Compos.* **2014**, *35*, 708–714. [[CrossRef](#)]
- Saiz-Arroyo, C.; Rodríguez-Pérez, M.A.; Tirado, J.; López-Gil, A.; Saja, J.A. Structure–property relationships of medium-density polypropylene foams. *Polym. Int.* **2013**, *62*, 1324–1333. [[CrossRef](#)]
- Chen, S.; Wang, C.; Li, J. Effect of alkyl groups in organic part of polyoxo-metalates based ionic liquids on properties of flame retardant polypropylene. *Thermochim. Acta* **2016**, *631*, 51–58. [[CrossRef](#)]

8. Rault, F.; Giraud, S.; Salaün, F.; Almeras, X. Development of a halogen free flame retardant masterbatch for polypropylene fibers. *Polymers* **2015**, *7*, 220–234. [[CrossRef](#)]
9. Lomakin, S.M.; Dubnikova, I.L.; Berezina, S.M.; Zaikov, G.E. Thermal degradation and combustion of a polypropylene nanocomposite based on organically modified layered aluminosilicate. *Polym. Sci. Ser. A* **2006**, *48*, 72–84. [[CrossRef](#)]
10. Han, J.; Shimizu, T.; Wataru, M.; Kim, H.; Wang, G. Polypropylene combustion in a fluidized bed combustor. *Energ. Sources A* **2010**, *32*, 1121–1129. [[CrossRef](#)]
11. Tang, T.; Chen, X.; Meng, X.; Chen, H.; Ding, Y. Synthesis of multiwalled carbon nanotubes by catalytic combustion of polypropylene. *Angew. Chem.* **2005**, *117*, 1541–1544. [[CrossRef](#)]
12. Leem, S.; Lee, J.; Huh, Y. A study on the concentration of CO by the length and the variation of the bent tube of the exhaust pipe for a household gas boiler. *J. Mech. Sci. Technol.* **2008**, *22*, 1554–1560. [[CrossRef](#)]
13. Pappalardo, S.; Russo, P.; Acierno, D.; Rabe, S.; Schartel, B. The synergistic effect of organically modified sepiolite in intumescent flame retardant polypropylene. *Eur. Polym. J.* **2016**, *76*, 196–207. [[CrossRef](#)]
14. Feng, C.; Liang, M.; Jiang, J.; Huang, J.; Liu, H. Synergistic effect of a novel triazine charring agent and ammonium polyphosphate on the flame retardant properties of halogen-free flame retardant polypropylene composites. *Thermochim. Acta* **2016**, *627–629*, 83–90. [[CrossRef](#)]
15. Song, R.; Zhang, B.; Huang, B.; Tang, T. Synergistic effect of supported nickel catalyst with intumescent flame-retardants on flame retardancy and thermal stability of polypropylene. *J. Appl. Polym. Sci.* **2006**, *102*, 5988–5993. [[CrossRef](#)]
16. Lai, X.J.; Tang, S.; Li, H.Q.; Zeng, X.G. Flame-retardant mechanism of a novel polymeric intumescent flame retardant containing caged bicyclic phosphate for polypropylene. *Polym. Degrad. Stab.* **2015**, *113*, 22–31. [[CrossRef](#)]
17. Dittrich, B.; Wartig, K.; Mülhaupt, R.; Schartel, B. Flame-retardancy properties of intumescent ammonium poly (phosphate) and mineral filler magnesium hydroxide in combination with graphene. *Polymers* **2014**, *6*, 2875–2895. [[CrossRef](#)]
18. Cui, Z.; Qu, B. Synergistic effects of layered double hydroxide with phosphorus-nitrogen intumescent flame retardant in PP/EPDM/IFR/LDH nanocomposites. *Chin. J. Polym. Sci.* **2010**, *28*, 563–571. [[CrossRef](#)]
19. Chen, X.; Yu, J.; He, M.; Guo, S.; Luo, Z.; Lu, S. Effects of zinc borate and microcapsulated red phosphorus on mechanical properties and flame retardancy of polypropylene/magnesium hydroxide composites. *J. Polym. Res.* **2009**, *16*, 357–362. [[CrossRef](#)]
20. Haurie, L.; Fernández, A.I.; Velasco, J.I.; Chimenos, J.M.; Cuesta, J.L.; Espiell, F. Synthetic hydromagnesite as flame retardant. Evaluation of the flame behaviour in a polyethylene matrix. *Polym. Degrad. Stab.* **2006**, *91*, 989–994. [[CrossRef](#)]
21. Hippi, U.; Mattila, J.; Korhonen, M.; Seppälä, J. Compatibilization of polyethylene/aluminum hydroxide (PE/ATH) and polyethylene/magnesium hydroxide (PE/MH) composites with functionalized polyethylenes. *Polymer* **2003**, *44*, 1193–1201. [[CrossRef](#)]
22. Du, L.; Qu, B.; Meng, Y.; Zhu, Q. Structural characterization and thermal and mechanical properties of poly (propylene carbonate)/MgAl-LDH exfoliation nanocomposite via solution intercalation. *Compos. Sci. Technol.* **2006**, *66*, 913–918. [[CrossRef](#)]
23. Tsai, T.Y.; Shiu, W.C. Synthesis and Characterization of Poly(ethylene terephthalate)/modified lithium-aluminum-layered double hydroxide nanocomposites prepared using in-situ polymerization. *J. Chin. Chem. Soc.* **2014**, *61*, 891–896. [[CrossRef](#)]
24. Sahoo, P.; Ishihara, S.; Yamada, K.; Deguchi, K.; Ohki, S.; Tansho, M.; Shimizu, T.; Eisaku, N.; Sasai, R.; Labuta, J.; et al. Rapid exchange between atmospheric CO<sub>2</sub> and carbonate anion intercalated within magnesium rich layered double hydroxide. *ACS Appl. Mater. Interfaces* **2014**, *6*, 18352–18359. [[CrossRef](#)] [[PubMed](#)]
25. Nejati, K.; Davari, S.; Rezvani, Z.; Dadashzadeh, M. Adsorption of 4-chloro-2-methylphenoxy acetic acid (MCPA) from aqueous solution onto Cu-Fe-NO<sub>3</sub> layered double hydroxide nanoparticles. *J. Chin. Chem. Soc.* **2015**, *62*, 371–379. [[CrossRef](#)]
26. Wang, L.; Zhang, M.; Li, B. Thermal analysis and flame-retarded mechanism of composites composed of ethylene vinyl acetate and layered double hydroxides containing transition metals (Mn, Co, Cu, Zn). *Appl. Sci.* **2016**, *6*, 131. [[CrossRef](#)]

27. Wang, B.; Zhou, K.; Wang, B.; Gui, Z.; Hu, Y. Synthesis and characterization of CuMoO<sub>4</sub>/Zn–Al layered double hydroxide hybrids and their application as a reinforcement in polypropylene. *Ind. Eng. Chem. Res.* **2014**, *53*, 12355–12362. [[CrossRef](#)]
28. Gao, Y.; Wang, Q.; Wang, J.; Huang, L.; Yan, X.; Zhang, X.; He, Q.; Xing, Z.; Guo, Z. Synthesis of Highly Efficient Flame Retardant High-Density Polyethylene Nanocomposites with Inorgano-Layered Double Hydroxides as Nanofiller Using Solvent Mixing Method. *ACS Appl. Mater. Interfaces* **2014**, *6*, 5094–5104. [[CrossRef](#)] [[PubMed](#)]
29. Lonkar, S.P.; Therias, S.; Leroux, F.; Gardette, J.L.; Singh, R.P. Influence of reactive compatibilization on the structure and properties of PP/LDH nanocomposites. *Polym. Int.* **2011**, *60*, 1688–1696. [[CrossRef](#)]
30. Shabanian, M.; Basaki, N.; Khonakdar, H.A.; Jafari, S.H.; Hedayati, K.; Wagenknecht, U. Novel nanocomposites consisting of a semi-crystalline polyamide and Mg–Al LDH: Morphology, thermal properties and flame retardancy. *Appl. Clay Sci.* **2014**, *90*, 101–108. [[CrossRef](#)]
31. Tsai, T.Y.; Laio, J.R.; Naveen, B. Preparation and characterization of PET/LDH or clay nanocomposites through the microcompounding process. *J. Chin. Chem. Soc.* **2015**, *62*, 547–553. [[CrossRef](#)]
32. Wang, L.; Li, B.; Hu, Z.; Cao, J. Effect of nickel on the properties of composites composed of layered double hydroxides and ethylene vinyl acetate copolymer. *Appl. Clay Sci.* **2013**, *72*, 138–146. [[CrossRef](#)]
33. Wang, L.; Li, B.; Zhang, X.; Chen, C.; Zhang, F. Effect of intercalated anions on the performance of Ni–Al LDH nanofiller of ethylene vinyl acetate composites. *Appl. Clay Sci.* **2012**, *56*, 110–119. [[CrossRef](#)]
34. Wang, L.; Li, B.; Zhao, X.; Chen, C.; Cao, J. Effect of rare earth ions on the properties of composites composed of ethylene vinyl acetate copolymer and layered double hydroxides. *PLoS ONE* **2012**, *7*, e37781. [[CrossRef](#)] [[PubMed](#)]
35. Wang, L.; Li, B.; Yang, M.; Chen, C.; Liu, Y. Effect of Ni cations and microwave hydrothermal treatment on the related properties of layered double hydroxide–ethylene vinyl acetate copolymer composites. *J. Colloid Interface Sci.* **2011**, *356*, 519–525. [[CrossRef](#)] [[PubMed](#)]
36. Wang, W.; Pan, H.; Shi, Y.; Pan, Y.; Yang, W.; Liew, K.M.; Song, L.; Hu, Y. Fabrication of LDH nanosheets on β-FeOOH rods and applications for improving the fire safety of epoxy resin. *Compos. A Appl. Sci. Manuf.* **2016**, *80*, 259–269. [[CrossRef](#)]
37. Kalali, E.N.; Juan, S.D.; Wang, X.; Nie, S.; Wang, R.; Wang, D.Y. Comparative study on synergistic effect of LDH and zirconium phosphate with aluminum trihydroxide on flame retardancy of EVA composites. *J. Therm. Anal. Calorim.* **2015**, *121*, 619–626. [[CrossRef](#)]
38. Sandra, G.F.; Lorena, U.; Cristina, P.R.; Manuela, Z.; Corcuera, M.Á.; Eceiza, A. Flexible polyurethane foam nanocomposites with modified layered double hydroxides. *Appl. Clay Sci.* **2016**, *123*, 109–120.
39. Wang, D.Y.; Das, A.; Costa, F.R.; Leuteritz, A.; Wang, Y.Z.; Wagenknecht, U.; Heinrich, G. Synthesis of organo cobalt-aluminum layered double hydroxide via a novel single-step self-assembling method and its use as flame retardant nanofiller in PP. *Langmuir* **2010**, *26*, 14162–14169. [[CrossRef](#)] [[PubMed](#)]
40. Wang, D.Y.; Leuteritz, A.; Kutlu, B.; Landwehr, M.A.; Jehnichen, D.; Wagenknecht, U.; Heinrich, G. Preparation and investigation of the combustion behavior of polypropylene/organomodified MgAl-LDH micro-nanocomposite. *J. Alloys Compd.* **2011**, *509*, 3497–3501. [[CrossRef](#)]
41. Basile, F.; Benito, P.; Fornasari, G.; Vaccari, A. Hydrotalcite-type precursors of active catalysts for hydrogen production. *Appl. Clay Sci.* **2010**, *48*, 250–259. [[CrossRef](#)]
42. Ciuffi, K.J.; Nassar, E.J.; Rocha, L.A.; Rocha, Z.N.; Nakagaki, S.; Mata, G.; Trujillano, R.; Vicente, M.A.; Korili, S.A.; Gil, A. Preparation and characterization of new Ni-aluminosilicate catalysts and their performance in the epoxidation of (Z)-cyclooctene. *Appl. Catal. A Gen.* **2007**, *319*, 153–162. [[CrossRef](#)]
43. Herrero, M.; Benito, P.; Labajos, F.M.; Rives, V. Stabilization of Co<sup>2+</sup> in layered double hydroxides (LDHs) by microwave-assisted ageing. *J. Solid State Chem.* **2007**, *180*, 873–884. [[CrossRef](#)]
44. Wang, B.; Williams, G.R.; Chang, Z.; Jiang, M.; Liu, J.; Lei, X.; Sun, X. Hierarchical NiAl layered double hydroxide/multiwalled carbon nanotube/nickel foam electrodes with excellent pseudocapacitive properties. *ACS Appl. Mater. Interfaces* **2014**, *6*, 16304–16311. [[CrossRef](#)] [[PubMed](#)]
45. Benito, P.; Labajos, F.M.; Rocha, J.; Rives, V. Influence of microwave radiation on the textural properties of layered double hydroxides. *Microporous Mesoporous Mater.* **2006**, *94*, 148–158. [[CrossRef](#)]
46. Palmer, S.J.; Soisonard, A.; Frost, R.L. Determination of the mechanism(s) for the inclusion of arsenate, vanadate, or molybdate anions into hydrotalcites with variable cationic ratio. *J. Colloid. Interface Sci.* **2009**, *329*, 404–409. [[CrossRef](#)] [[PubMed](#)]

47. Arizaga, G.G.C.; Wypych, F.; Barraza, F.C.; Lopez, O.E.C. Reversible intercalation of ammonia molecules into a layered double hydroxide structure without exchanging nitrate counter-ions. *J. Solid State Chem.* **2010**, *183*, 2324–2328. [[CrossRef](#)]
48. Zhan, M.; Chen, G.; Wei, Z.; Shi, Y.; Zhang, W. Nonisothermal crystallization and morphology of poly(butylene succinate)/layered double hydroxide nanocomposites. *Chin. J. Polym. Sci.* **2013**, *31*, 187–200. [[CrossRef](#)]
49. Qiu, L.; Chen, W.; Qu, B. Morphology and thermal stabilization mechanism of LLDPE/MMT and LLDPE/LDH nanocomposites. *Polymer* **2006**, *47*, 922–930. [[CrossRef](#)]
50. Peacock, R.D.; Reneke, P.A.; Averill, J.D.; Bukowski, R.W.; Klote, J.H. Fire safety of passenger trains; phase II: Application of fire hazard analysis techniques. *Natl. Inst. Stand. Technol.* **2002**, 1–185.
51. Marzena, P.; Jerzy, G.; Zbignev, K. Investigation into the influence of flame retardant additives on some fire properties of polyester materials applying small-scale testing techniques. *J. Civ. Eng. Manag.* **2013**, *19*, 561–572.
52. Liu, L.; Zhang, H.; Sun, L.; Kong, Q.; Zhang, J. Flame-retardant effect of montmorillonite intercalation iron compounds in polypropylene/aluminum hydroxide composites system. *J. Therm. Anal. Calorim.* **2016**, *124*, 807–814. [[CrossRef](#)]
53. Jiao, C.; Chen, X. Synergistic effects of titanium dioxide with layered double hydroxides in EVA/LDH composites. *Polym. Eng. Sci.* **2011**, *51*, 2166–2170. [[CrossRef](#)]
54. Du, B.; Guo, Z.; Fang, Z. Effects of organo-clay and sodium dodecyl sulfonate intercalated layered double hydroxide on thermal and flame behaviour of intumescent flame retarded polypropylene. *Polym. Degrad. Stabil.* **2009**, *94*, 1979–1985. [[CrossRef](#)]
55. Kiliaris, P.; Papaspyrides, C.D. Polymer/layered silicate (clay) nanocomposites: An overview of flame retardancy. *Prog. Polym. Sci.* **2010**, *35*, 902–958. [[CrossRef](#)]
56. Dong, M.; Gu, X.; Zhang, S. Effects of compound oxides on the fire performance of polypropylene composite. *Ind. Eng. Chem. Res.* **2014**, *53*, 8062–8068. [[CrossRef](#)]
57. Jiang, S.D.; Bai, Z.M.; Tang, G.; Song, L.; Stec, A.A.; Hull, T.R.; Hu, Y.; Hu, W.Z. Synthesis of mesoporous silica@Co-Al layered double hydroxide spheres: Layer-by-layer method and their effects on the flame retardancy of epoxy resins. *ACS Appl. Mater. Interfaces* **2014**, *6*, 14076–14086. [[CrossRef](#)] [[PubMed](#)]



© 2017 by the authors; licensee MDPI, Basel, Switzerland. This article is an open access article distributed under the terms and conditions of the Creative Commons Attribution (CC-BY) license (<http://creativecommons.org/licenses/by/4.0/>).